Publishing House
AKAPIT

COMPUTER METHODS IN MATERIALS SCIENCE

Informatyka w Technologii Materiałów

Vol. 9, 2009, No. 4

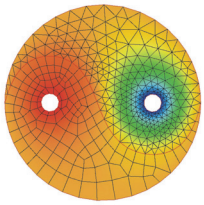

VALIDATION OF THE THERMO-MECHANICAL-MICROSTRUCTURAL MODEL OF HOT FORGING PROCESS

ROMAN KUZIAK[1]*, VALERIY PIDVYSOTS'KYY[1], KRZYSZTOF DROZDOWSKI[2]

[1)] Institute for Ferrous Metallurgy, K. Miarki 12, 44-100 Gliwice, Poland
[2)] Zakład Obróbki Plastycznej Sp. z o.o., ul. Kuźnicza 13, 21-045 Świdnik k/Lublina
**Corresponding Author: RomanKuziak@imz.pl*

Abstract

The paper deals with mathematical modelling of non-isothermal forging process accounting for the distribution of effective strain, strain rate, temperature and microstructural changes occurring in the deformed material. So far, forging technologies of the investigated alloyed steel grade 16NCD13 have been designed intuitively and applied in practice, but there is still lack of reliable models describing behaviour of this steel during thermomechanical processing. Thus, the general objective of the present work was to develop rheological and microstructure evolution model for the steel under investigation. Uniaxial compression tests were performed in a wide range of strains, strain rates and temperatures. The experimental results, in the form of load vs. displacement measurements, were used as input for the inverse calculations. Rheological models based on flow stress functions of various complexity were determined and validated. It is shown that when the inverse analysis is applied to the interpretation of the plastometric tests, the properties of the material are insensitive to the method of testing and to the sample dimensions. A number of tests with identical deformation conditions and various intervals between deformation and quenching were performed to provide data for identification of the microstructure evolution model. Also stress relaxation technique was used for this purpose. The models were implemented into Forge2008 commercial code for the simulation of industrial forging process. The results of the simulation show good predictive ability of combined thermal-mechanical-microstructure evolution model in hot forging of 16NCD13 steel

Key words: rheological model, microstructure evolution model, finite element method, plastometric tests, numerical simulation, forging process

1. INTRODUCTION

Alloyed steels, which are characterised by interesting mechanical properties after heat treatment, have become more and more often used in industrial applications. On the other hand, there is still lack of models, which allow the simulation of behaviour of these steels during processing. Such models would be helpful in designing the forming technology and would supply information useful in process optimization. The role of modelling has become even more important when the idea of comprising the whole manufacturing chains has become introduced (Madej et al., 2007; Bariani et al., 2007). Technology design based on the optimization of the whole manufacturing chain is, from one side very promising and high advantages are expected, but from the other side it requires advanced models capable of simulating of production chains.

Accuracy of numerical simulations of metal forming processes depends, to a large extent, on the correctness of description of material rheological properties as well as mechanical and thermal boundary conditions. The former aspect related to the 16NCD13 steel is the topic of the present work. The first objective of the project is evaluation of the rheological parameters in various conditions of deformation by performing plastometric tests. Inverse

 ISSN 1641-8581

analysis (Szeliga et al., 2006a) is applied to eliminate the influence of inhomogeneities of strains, effect of friction and heat generated due to deformation and due to friction which are the main disturbances in the tests.

Identification of the microstructure evolution model is the second objective of the work. Microstructure of samples was investigated after each test and the data for identification of the microstructure evolution model was supplied. Connection of the rheological and microstructure evolution models with the finite element program was the third objective for the industrial forging process simulation.

The simulation of industrial forging process was conducted to validate the thermo-mechanical-microstructural model developed in this project.

2. EXPERIMENTS

Uniaxial compression tests were performed on cylindrical samples having dimensions ϕ10×12 mm to develop the constitutive equation and microstructure evolution model. The experimental steel contained: 0.14%C, 0.5%Mn, 0.29%Si, 0.98%Cr, 3.10%Ni, 0.002%Ti and 0.005%N. The deformation tests were performed on the Gleeble 3800 simulator at the IMZ Gliwice (Poland), at temperatures 850, 900, 1000, 1100 and 1150°C and at constant strain rates 0.1, 1, 20, 100 and 200 s^{-1} for each temperature. Loads were recorded in each test as a function of the die displacement. The measured barrelling of the sample after compression was an input for the inverse analysis, which yielded average friction coefficient of 0.14 for all the tests. The low value of the friction coefficient is connected with the use of graphite and tantalum foils and anti-seize compound (Nickel) as lubricant between specimen and anvils.

Three sets of experiments were performed. The first set with the strain of 1 was performed to identify the rheological model. Typical load-displacement data obtained in these tests are shown in figure 1. The remaining two sets of tests were performed to supply the data for the microstructure evolution model. The objective of the second set of tests was to investigate influence of the preheating time on the microstructure prior to deformation. The objective of the third set of tests was identification of the microstructure evolution model. The procedure for each set of the tests is given in table 1.

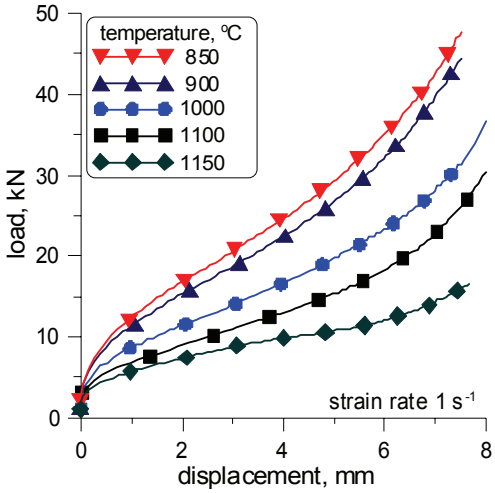

***Fig. 1**. Measured load-displacement relation during uniaxial compression of experimental steel at various temperatures and strain rate 1 s^{-1}.*

***Table 1.** Procedure in the three sets of tests (Q – quenching).*

Set	Preheating temperature °C	Heating rate °C/s	Preheating time s	Cooling rate °C/s	Maintaining at test temperature s	Strain	Cooling rate °C/s
I	1150	3	120	5	60	1.0	water
II	1150	3	60	5	30	1.0	water
III	850-950	3	0-1800	Q	-	-	-

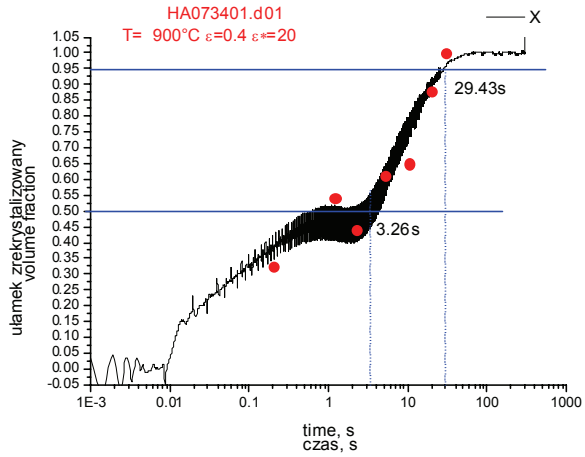

***Fig. 2**. Comparison of the softening curves determined in the double deformation tests (red dots) and in the stress relaxation experiments (continuous line).*

The double deformation and stress relaxation tests were conducted to develop the austenite microstructure evolution model. The methodology of these tests is described in publication (Karjalainen and Perttula, 1996). A comparison of these both methods in the determination of the softening coefficient is given in figure 2 for tests conducted at 900°C in which the samples were deformed to the strain 0.4 at

a strain rate 20 s^{-1}. Both methods compare fairly well. A plateau in the softening curve is associated with the suppression of static recrystallization by the TiC particles precipitation.

Samples were quenched after deformation at different stages of austenite microstructure evolution progression and the recrystallized volume fraction and grain size were measured for the model development.

3. INVERSE ANALYSIS

Details of the inverse algorithm, which is used for rheological model development, are described by Pietrzyk (2000). Briefly, the rheological and friction parameters are determined by searching for a minimum of a goal function:

$$\phi = \sqrt{\frac{1}{Nt}\sum_{i=1}^{Nt}\left[\frac{1}{Nr}\sum_{j=1}^{Nr}\left(\frac{R_{ij}^m - R_{ij}^c}{R_{ij}^m}\right)^2 + \frac{1}{Ns}\sum_{j=1}^{Ns}\left(\frac{F_{ij}^m - F_{ij}^c}{F_{ij}^m}\right)^2\right]} \tag{1}$$

where: Nt – number of tests, Nr – number of radius measurements along the height of the sample, Ns – number of load measurement sampling points in one test, F_{ij}^m, F_{ij}^c – measured and calculated load, respectively, R_{ij}^m, R_{ij}^c – measured and calculated radius of the sample after the test, respectively.

Goal function (1) is used for the uniaxial compression tests. Both, friction coefficient and flow stress model are determined from these tests (Szeliga et al., 2006a). Calculated values of loads and shape of the samples are obtained from the direct problem model. This model is based on the rigid-plastic thermo-mechanical finite element solution presented by Lee and Kobayashi (1973). Detailed description of the algorithm and the program, which are used in this work, is given in (Kobayashi et al., 1989). The main equations are repeated below briefly for completeness. The solution assumes that the material obeys Huber-Mises yield criterion and associated Levy-Mises flow rule. The velocity field is calculated by searching for a minimum of the power functional:

$$J = \int_\Omega \left(\sigma_i \dot{\varepsilon}_i + \lambda \dot{\varepsilon}_V\right) d\Omega - \int_\Gamma \mathbf{f}^T \mathbf{v}_s d\Gamma \tag{2}$$

where: σ_i – effective stress, which is equal to the flow stress σ_p, $\dot{\varepsilon}_i$ – effective strain rate, Ω – volume, Γ – contact surface, $\dot{\varepsilon}_V$ – volumetric strain rate, λ – Lagrange multiplier, $\mathbf{f}$ – vector of boundary tractions, $\mathbf{v}_s$ – vector of slip velocities.

In the flow theory of plasticity, strain rates are related to stresses by the Levy-Mises flow rule, see eg. (Kobayasi et al., 1989). Flow stress σ_p in equation (2) is the only one material parameter in the model. This parameter is, however, dependent on a number of process parameters such as strain, strain rate and temperature. Determination of the function describing these relations is the main objective of the inverse analysis.

The flow formulation, which is the basis of the mechanical model, is coupled with the finite element solution of the Fourier heat transfer equation:

$$\nabla k(T)\nabla T + Q(T) = c_p(T)\rho(T)\frac{\partial T}{\partial t} \tag{3}$$

where: $k(T)$ – conductivity, $Q(T)$ – heat generation rate due to deformation work, $c_p(T)$ – specific heat, $\rho(T)$ – density, T – temperature, t – time.

The following boundary conditions are used in the solution:

$$k\frac{\partial T}{\partial \mathbf{n}} = q + \alpha\left(T_a - T\right) \tag{4}$$

where: α – heat transfer coefficient, T_a – surrounding temperature or tool temperature, q – heat flux due to friction, $\mathbf{n}$ – unit vector normal to the surface.

Discretization of the problem is performed in a typical finite element manner and simulations of metal forming processes can be performed.

Friction plays an important role in the inverse analysis of plastometric tests. The friction model suggested first by Chen and Kobayashi (1978), is used in the FE code:

$$\tau = m\sigma_p \frac{2}{\pi}\operatorname{arctg}\frac{\Delta v}{a} \tag{5}$$

where m – friction coefficient, Δv – relative slip velocity, a – a constant, few orders smaller than an average slip velocity.

4. RESULTS

4.1. Rheological Model

Results of the inverse analysis for all the tests are presented in figure 3 in terms of corrected stress-strain curves.

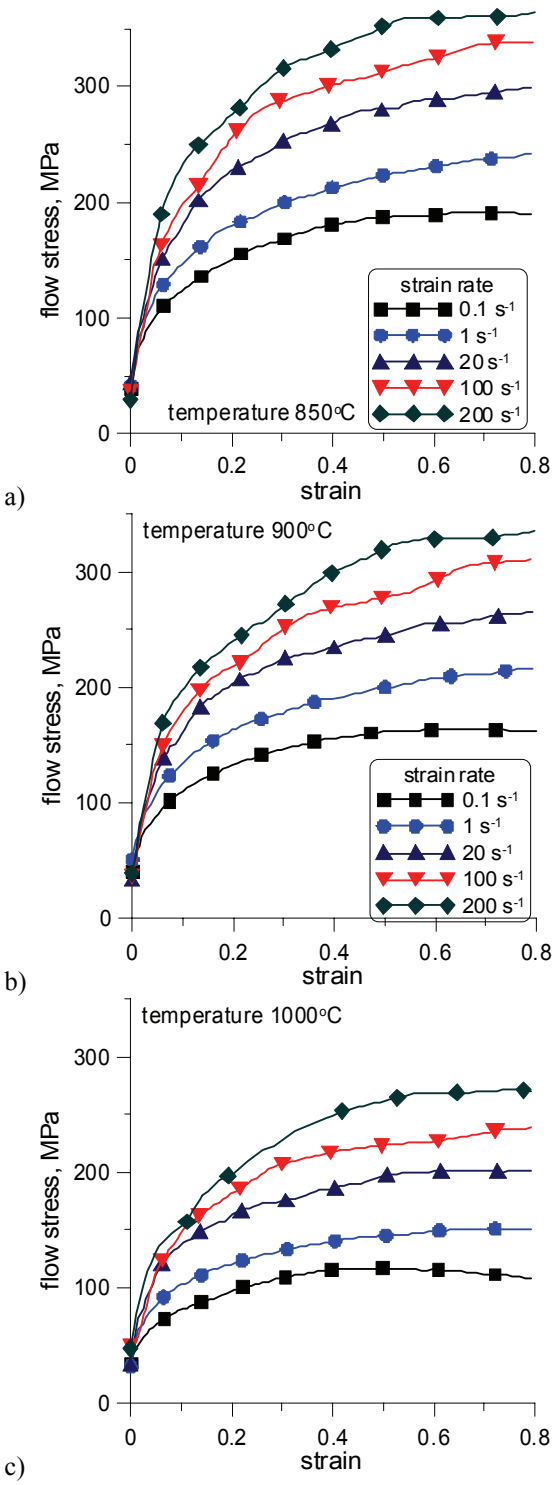

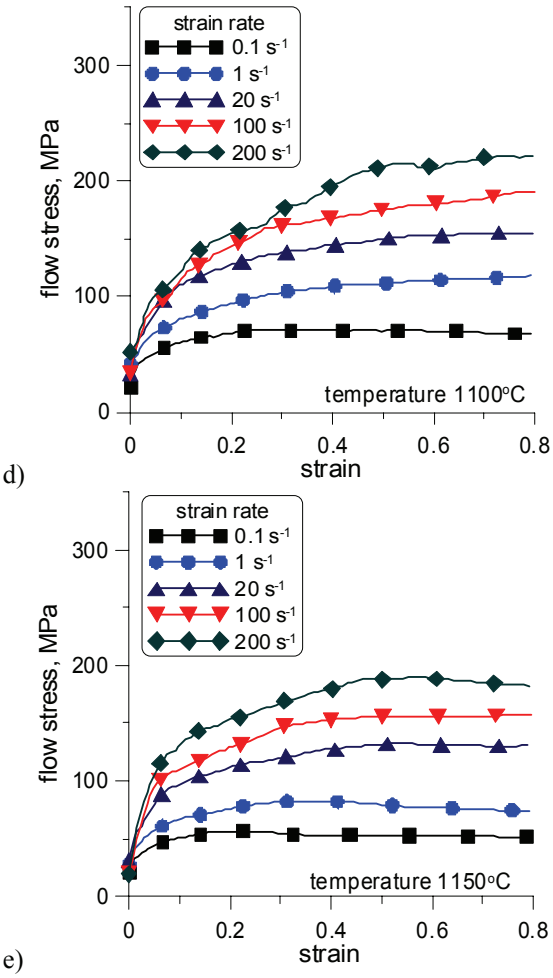

***Fig. 3**. Flow stress of the experimental steel determined using inverse analysis for various strain rates and temperatures 850°C (a), 900°C (b), 1000°C (c), 1100°C (d) and 1150°C (e).*

Analysis of results presented in figure 3 shows that that dynamic recrystallization (DRX) occurs for low values of the Zener-Hollomon parameter, therefore, selection of the flow stress function has to be constrained to those models, which can account for the material softening during deformation. A number of functions describing relation between flow stress and process parameters in the conditions of DRX have been proposed and some of them are discussed by Grosman (1997). In the present work, however, reasonably simple function described by Gavrus et al. (1996) was selected first:

$$\sigma_p = \sqrt{3}\left[WK_0\varepsilon^n \exp\left(\frac{\beta}{T}\right) + (1-W)K_s \exp\left(\frac{\beta_s}{T}\right)\right]\left(\sqrt{3}\dot{\varepsilon}\right)^m \quad (6)$$

where: $W = \exp(-R_0\varepsilon)$

K_0, n, β, K_s, β_s, m, R_0 in equation (6) are material parameters, which are determined using the inverse analysis.

Equation (6) describes quite well the flow stress when the effect of softening due to dynamic recrystallization is not complicated. In some materials, however, dynamic recrystallization leads to fast softening after the peak strain and then the steady state is reached, when constant saturation stress is maintained. This problem is well researched by (Szeliga et al., 2006b). The equation (model D-S), which is much more flexible in description of materials softening, was developed at the University of Sheffield (Davenport et al., 1999):

$$\sigma_p = \sigma_0 + \left(\sigma_{ss(e)} - \sigma_0\right)\left[1 - \exp\left(-\frac{\varepsilon}{\varepsilon_r}\right)\right]^{\frac{1}{2}} - R \quad (7)$$

where:

$$R = \begin{cases} 0 & \varepsilon \le \varepsilon_c \\ \left(\sigma_{ss(e)} - \sigma_{ss}\right)\left\{1 - \exp\left[-\left(\frac{\varepsilon - \varepsilon_c}{\varepsilon_{xr} - \varepsilon_c}\right)^2\right]\right\} & \varepsilon > \varepsilon_c \end{cases}$$

$$\sigma_0 = \frac{1}{\alpha_0}\sinh^{-1}\left(\frac{Z}{A_0}\right)^{\frac{1}{n_0}},$$

$$\sigma_{ss(e)} = \frac{1}{\alpha_{sse}}\sinh^{-1}\left(\frac{Z}{A_{sse}}\right)^{\frac{1}{n_{sse}}},$$

$$\sigma_{ss} = \frac{1}{\alpha_{ss}}\sinh^{-1}\left(\frac{Z}{A_{ss}}\right)^{\frac{1}{n_{ss}}},$$

$$\varepsilon_r = 0.31\left[q_1 + q_2(\sigma_{ss(e)})^2\right], \qquad \varepsilon_{xr} - \varepsilon_c = \frac{\varepsilon_{xs} - \varepsilon_c}{1.98},$$

$$\varepsilon_c = C_c\left(\frac{Z}{\sigma_{ss(e)}^2}\right)^{N_c}, \quad \varepsilon_{xs} - \varepsilon_c = C_x\left(\frac{Z}{\sigma_{ss(e)}^2}\right)^{N_x}$$

This equation is described also in (Kowalski et al., 2000). It allows for modelling the variety of materials behavior during deformation in a wide range of deformation conditions. The main difficulty in application of this model is the large number of parameters, which have to be identified. Nevertheless, equation (6) was also examined in the present work.

The conventional flow stress models are based on the assumption that stress σ_p depends on plastic strain ε, and on the external process parameters (e.g., temperature, strain rate), which are grouped in the vector **p**: ($\sigma_p = f(\varepsilon,\mathbf{p})$). The main drawback of this approach is that it does not account for the history of deformation. Whenever the conditions of deformation change, the calculated material response immediately moves to a new equation of state and the flow stress depends only on the current new values of the strain and the external variables. In real deformation processes of steels some delay in the material response is possible. This delay depends on the chemical composition and it is connected with various microstructural phenomena that take place during deformation. Thus, the internal variable model (IVM) is often used. It allows more accurate description of the material transient behaviour. In this approach, stress is a function of time t; again of some external process variables (e.g., temperature, strain rate), which are grouped in the vector **p**, and internal variables, which are grouped in the vector **q**: ($\sigma_p = f(t,\mathbf{q},\mathbf{p})$).

Usually only one internal variable is considered for metallic materials, the average dislocation density, ρ. The flow stress in this model is proportional to the square root of the average dislocation density according to the formula:

$$\sigma_p = \sigma_0 + \alpha b \mu \sqrt{\rho} \quad (8)$$

where: σ_0 – stress due to elastic deformation, μ – shear modulus, α – constant.

The evolution of the dislocation density during deformation is described by the following general equation:

$$\frac{d\rho(t)}{dt} = \frac{\dot{\varepsilon}}{bl} - k_2\rho(t) - \frac{k_3}{D}\rho(t)\mathrm{R}\left[\rho(t) - \rho_{cr}\right] \quad (9)$$

where: $\rho(t)$ – dislocation density, t – time, b – Burgers vector, D – grain size, ρ_{cr} – critical dislocation density, calculated as a function of the Zener-Hollomon parameter, l – mean free path of dislocations, calculated as:

$$l = a_0 Z^{-a_1}$$

Function R in equation (10) is calculated as:

$$\mathrm{R}[\rho(t) - \rho_{cr}] = 0 \qquad \text{for } \rho \le \rho_{cr}$$

$$\mathrm{R}[\rho(t) - \rho_{cr})] = \rho\,(t - t_{cr}) \qquad \text{for } \rho > \rho_{cr}$$

where: t_{cr} – time at the beginning of dynamic recrystallization.

Parameters A_3 and k_2 are defined by Arrhenius law with coefficients A_{30} and k_{20} and activation energies of grain boundary mobility Q_m and self-diffusion Q_s, respectively:

$$k_2 = k_{20}\exp\left(\frac{Q_s}{RT}\right) \qquad k_3 = k_{30}\exp\left(\frac{Q_m}{RT}\right) \quad (10)$$

The advantage of the internal variable method is that it takes into account the history of deformation and is capable of predicting the delay in response due to different processes that take place during deformation. Model ability for prediction material behaviour during hot deformation has been experimentally proved in (Ordon et al., 2000). These studies under varying conditions (varying temperatures

and strain rates) of deformation confirmed the model qualitative predictive capability.

In order to simulate complex microstructural phenomena, the dislocation density cannot be treated as an average value in the model. The dislocation distribution function $G(\rho,t)$ suggested in (Sandstrom & Lagneborg, 1975) and defined as a volume fraction with a dislocation density between ρ and $\rho + d\rho$, is used to describe the phenomena in the alloy during hot plastic deformation. An average value of ρ, which is calculated as a weighted average of $G(\rho,t)$, is used to determine the flow stress from equation (8). The details of the numerical procedure are given by Pietrzyk (1994).

Coefficients in the three investigated rheological models obtained using inverse analysis of the tests for 16NCD13 steel are given in table 2. Additionally, activation energy in the Zener-Hollomon parameter in the D-S model, equation (7), was determined as Q_{def} = 377000 J/mol. Final value of the cost function (1), which represents accuracy of the inverse solution, is also given in table 2 for each model.

$$\varepsilon_m = p_5 d_0^{\,p_6} Z^{p_7} \tag{13}$$

where ε_p is the peak strain, d_0 is initial grain size, Z is Zener-Hollomon parameter, p_1 -p_7 are coefficients.

The dynamically recrystallized volume fraction is expressed by the following relationship:

$$X_{dyn} = 1 - \exp\left(p_8 \left(\frac{\varepsilon - \varepsilon_c}{\varepsilon_s - \varepsilon_c} \right)^{p_9} \right) \tag{14}$$

The dynamically recrystallized grain size is calculated with the following equation:

$$d_{rec}^{dyn} = p_{10} Z^{p_{11}} \tag{15}$$

To predict the static recrystallization kinetics, the Avrami's equation has been used in the following form:

$$X_{st} = 1 - \exp\left(-\ln(0.5) \left[\frac{t}{t_{0.5}^{st}} \right]^{1.7} \right) \tag{16}$$

where time $t_{0.5}^{st}$ for finishing 50% recrystallization is expressed as:

Table 2. *Coefficients in the rheological models determined using inverse analysis.*

eq.	K_0 MPa	n	β K	K_s MPa	β_s K	m	R_0	Φ
(6) CEMEF	4.93	0.398	4212.4	0.0363	7227.4	0.102	0.6775	0.129
eq.	A_0	n_0	α_0	A_{sse}	n_{sse}	α_{sse}	A_{ss}	n_{ss}
	0.45×10^{13}	45.16	0.0457	0.249×10^{12}	5.355	0.0099	0.565×10^{13}	6.74
(7)	α_{ss}	q_1	q_2	C_c	N_c	C_x	N_x	Φ
D-S model	0.0099	0.908	0.12×10^{-10}	0.42×10^{-3}	0.0218	0.002	0.366	0.068
eq.	σ_0	a_0	a_1	k_{20}	k_{30}	Q_s	Q_m	Φ
(8) IVM	3.5	0.156×10^{-3}	0.16	100	1.83	33.6	401	0.052

4.2. Microstructure evolution model

Conventional approach to microstructure evolution modeling was adopted in this research (Sellars, 1979). The critical strain for the dynamic recrystallization to occur is expressed with the following equation:

$$\varepsilon_c = p_1 \varepsilon_p \tag{11}$$

The strain for the steady state attainment and strain to the peak are given with the following equations:

$$\varepsilon_s = p_2 d_0^{\,p_3} Z^{p_4} \tag{12}$$

$$t_{0.5}^{st} = A \varepsilon^{n_\varepsilon} \dot{\varepsilon}^{n_{\dot\varepsilon}} D_0 \exp\left(\frac{Q}{RT} \right) \tag{17}$$

The austenite grain size upon the static recrystallization completion is calculated with the following equation:

$$D_{rec}^{st} = A \varepsilon^{n_\varepsilon} \dot{\varepsilon}^{n_{\dot\varepsilon}} D_0^{n_d} \exp\left(-\frac{Q}{RT} \right) \tag{18}$$

The following equations were used for the calculation of grain growth kinetics after the recrystallization completion:

$$D^{10.37} = D_0^{10.37} + \left(7.71\times10^{33}\right)\exp\left(-\frac{555663}{RT}\right)t \qquad T \le 1228\ K$$
$$D^{4.72} = D_0^{4.72} + \left(7.13\times10^{19}\right)\exp\left(-\frac{345000}{RT}\right)t \qquad T > 1228\ K \tag{19}$$

Time in the equation is given in seconds, temperature in Kelvins, and grain size in μm. The microstructure evolution model coefficients are given in table 3 trough 5.

Table 3. *Coefficients in the dynamic recrystallization model.*

p_1	p_2	p_3	p_4	p_5	p_6
0.8	$4.405\ 10^{-4}$	0.3043	0.1998	$4.531\ 10^{-4}$	-0.0253
p_7	p_8	p_9	p_{10}	p_{11}	
0.2431	-0.1763	1.813	152.16	-0.05238	

Table 4. *Coefficients in the static recrystallization kinetics model.*

n	A	n_ε	$n_{\dot\varepsilon}$	n_d	Q
0.651	$7.155\cdot10^{-7}$	-0.1883	-0.3753	0.822	109200

Table 5. *Coefficients in the equation for static grain size.*

A	n_ε	$n_{\dot\varepsilon}$	n_d	Q
$2.21\cdot10^{-12}$	-0.908	-0.0422	2.122	200 000

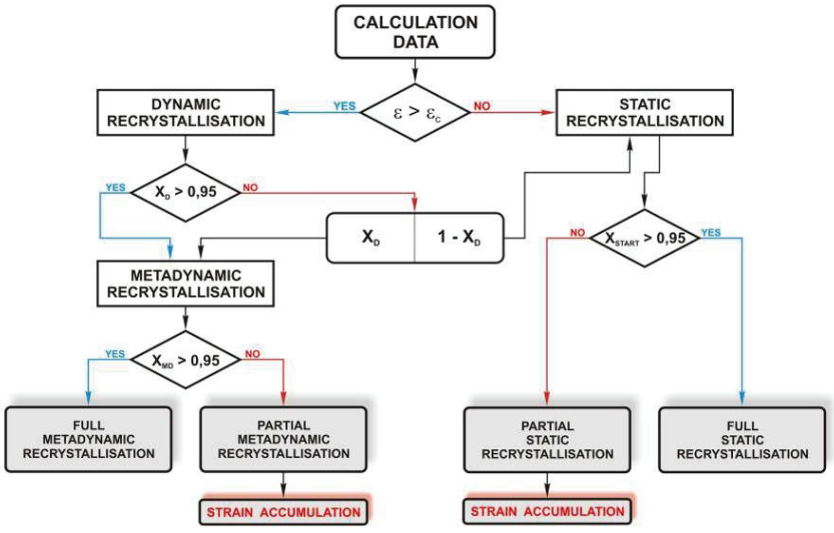

Fig. 4. *Algorithm of the austenite microstructure evolution simulation in hot deformation.*

The developed model was implemented into Forge 3D commercial code for the simulation of forging of experimental steel. The general schematic of the numerical algorithm for the austenite microstructure evolution simulation during the rolling process is shown in figure 4.

The calculation of the effective strain after initiation of the recrystalization process in a material was performed using the following relation:

$$\varepsilon_r^i = \left(\varepsilon_r^{i-1} + \varepsilon^i\right)\left(1 - X_{st}^i\right) \tag{20}$$

where i is current pass deformation, ε_r^{i-1} is cumulative strain after preceding deformations ($i = 1 - \varepsilon_r^{i-1} = 0$), ε^i is current deformation, X_{st}^i is volume fraction of recrystallized material.

4.3. Simulation of forging process

Simulation of the production of selected forging was conducted to validate the microstructure evolution model using Forge2008 commercial code (FORGE 2008 Documentation, 2008). In the production process, the cylinder having dimensions ∅70×103 mm is soaked at 1150°C, and then upset to the height of 55 mm. Next, the workpiece is forged in two dies to reach the final shape. After each blow, the forged part was removed from the dies for descaling and greasing. Therefore, the intervals between subsequent deformations were 4-5 seconds. After the last blow, the forging is cut off at the circumference to achieve the proper dimensions and subsequently subject to heat treatment. The successive stages of the process are shown schematically in figure 5.

The initial austenite grain size (mean linear intercept) for the simulation was taken 60 μm. This size was estimated in the cylinder subject to heating in industrial furnace followed by water cooling. For the sake of the illustration of model prediction, the distributions of temperature, strain, and austenite grain size during three-pass forging in the finish die, 20 seconds after the last deformation, is shown in figure 6. In one trial of the industrial experiments, the forged part was subject to water quenching after 20-second interval elapsing from the last blow. Therefore, the effective strain distribution in figure 6 is influenced by the recrystallization process, which is described by equation (20).

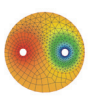

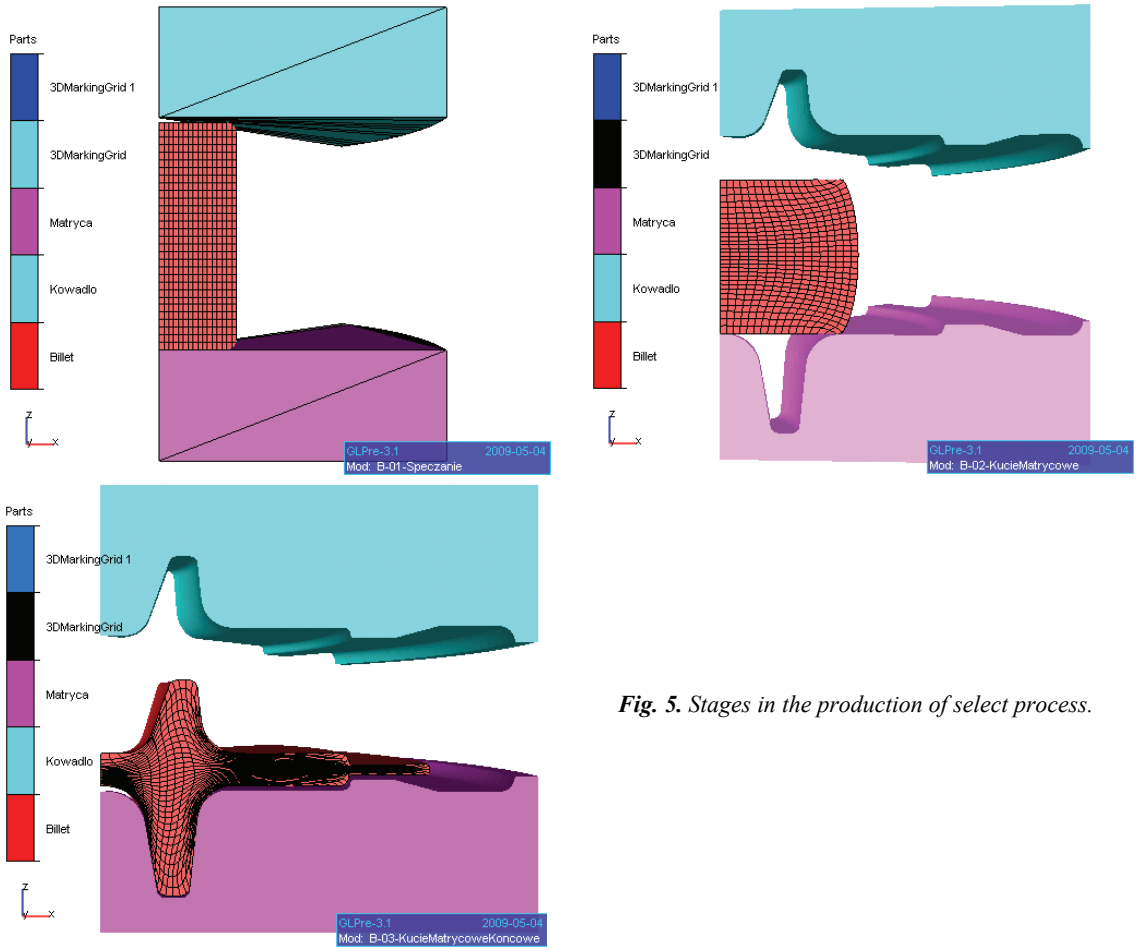

Fig. 5. *Stages in the production of select process.*

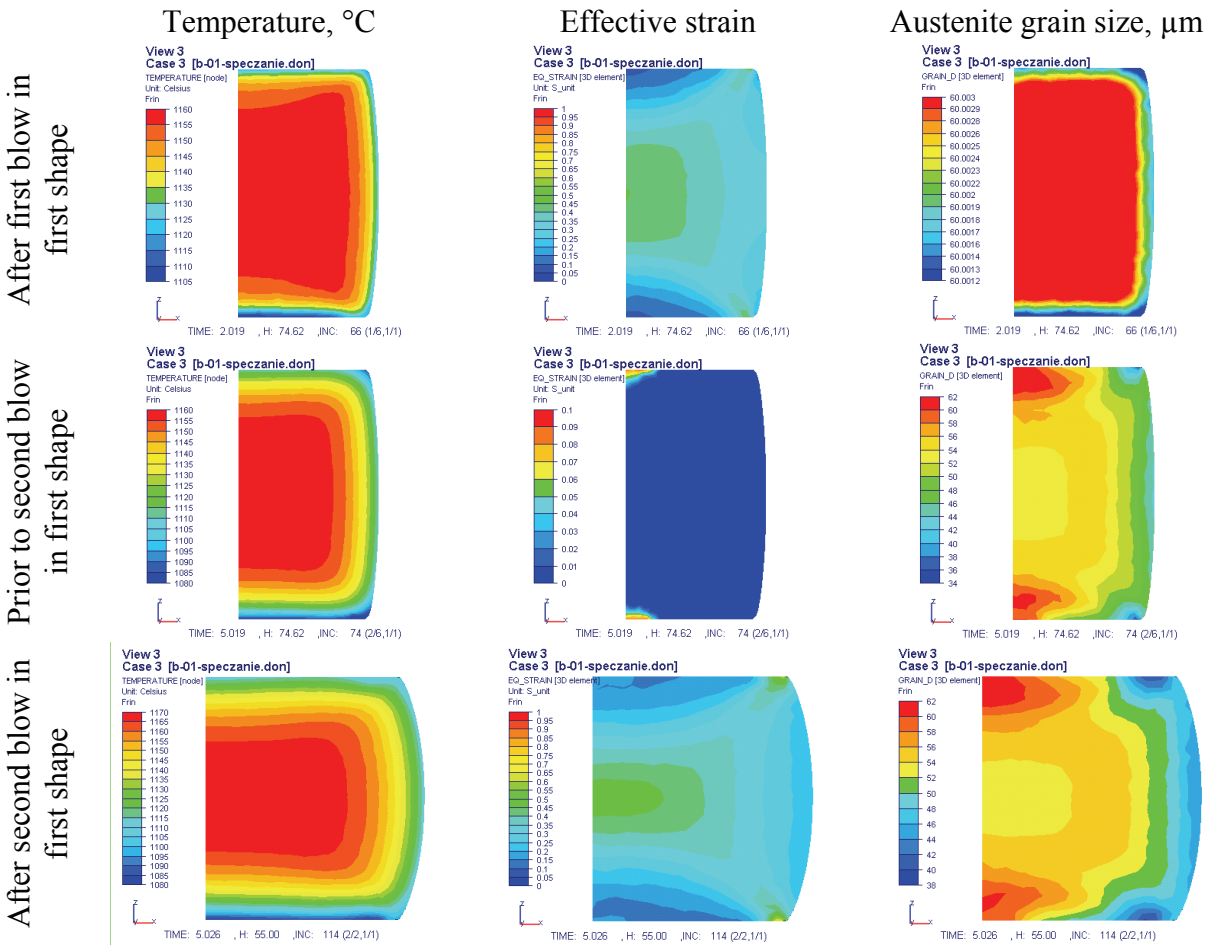

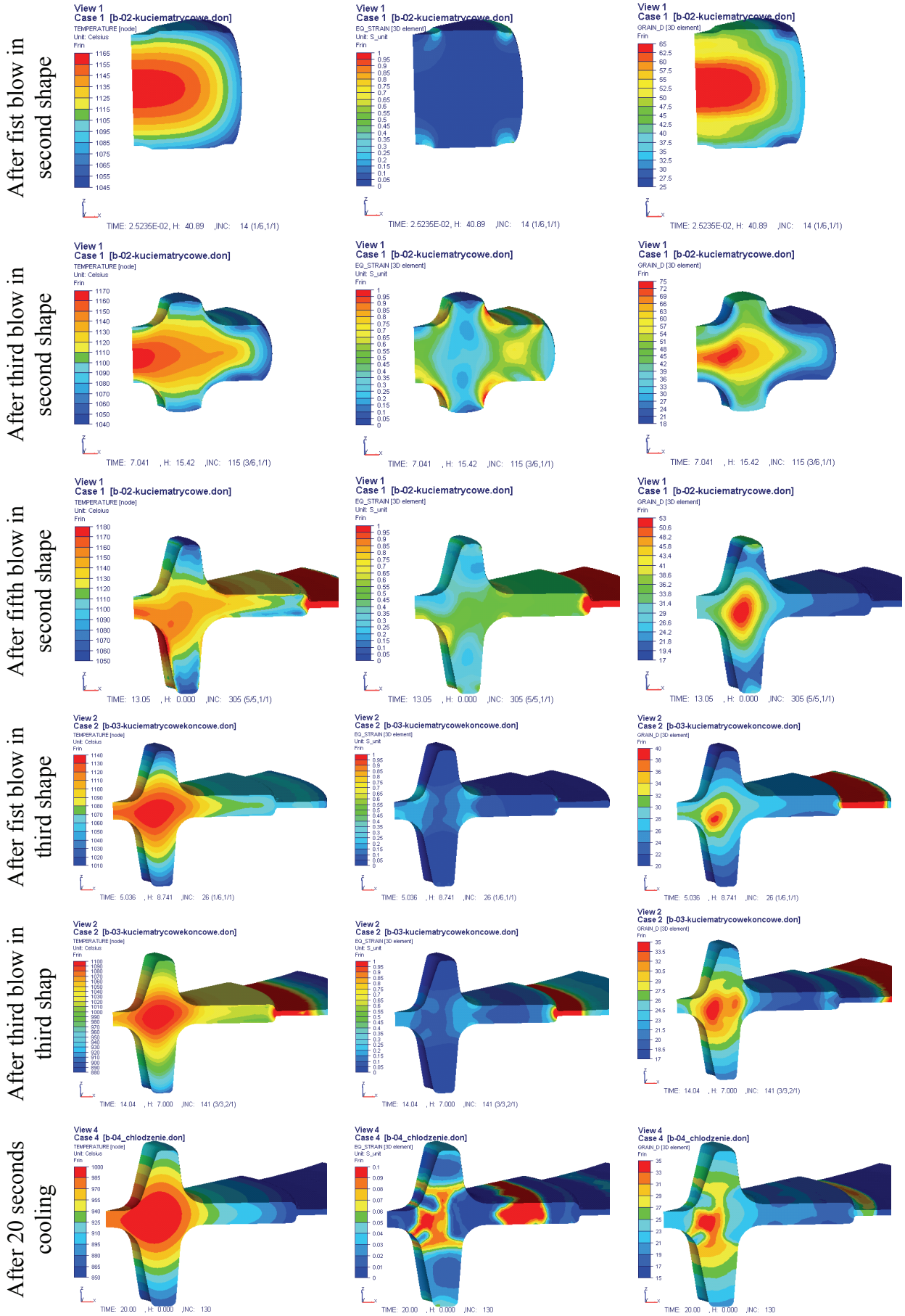

Fig. 6. *Distributions of: temperature, effective strain (with effect of recrystalization) and austenite grain size obtained in the numerical simulation of forging process.*

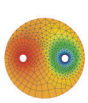

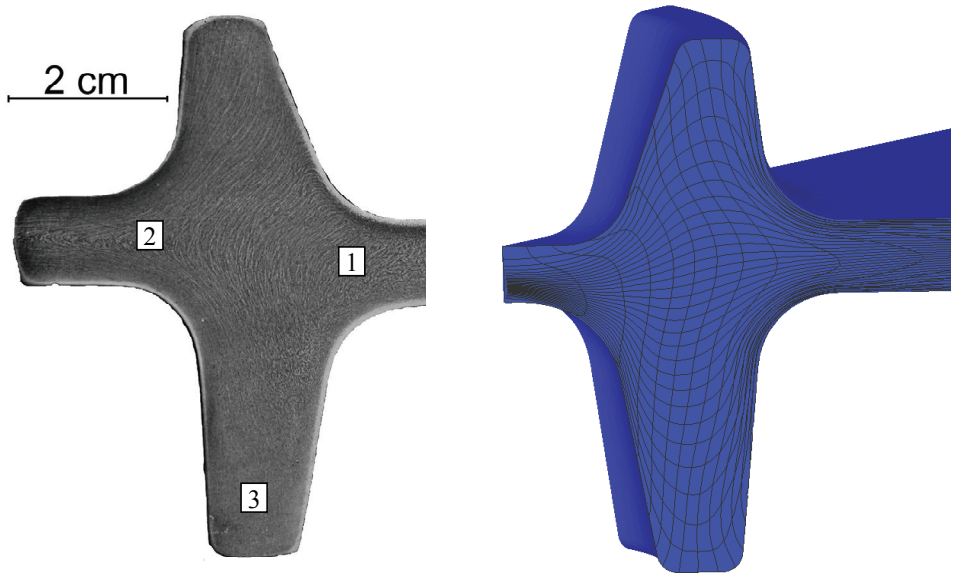

(a) (b)

Fig. 7. *Comparison plastic flow pattern – (a) with rectangular grid – (b).*

Verification of the model was conducted by comparing the result of the numerical simulation with the results of the metallographic examination. In figure 7, the shape of the grid obtained in the course of simulation was compared with the plastic flow lines pattern revealed by etching of the forging in the cross section plane, cut parallel to the axis of symmetry. One can see a good correspondence of the grid's geometry and the flow pattern. A good comparison was also obtained between calculated and measured austenite grain size (table 7).

Table 7. *Comparison of the calculated grain size with the results of measurement in areas "1", "2", and "3" marked in figure 7(a).*

Grain size μm	1	2	3
Measurement	22.5	20.8	22.9
Calculation	24.2	22.6	22.9

The result of the examination compares fairly well with the results of numerical calculation which suggests a good predictive capability of the developed models.

5. CONCLUSION

The application of inverse analysis allowed determination of the flow curves of alloyed steel which were not sensitive to the disturbances occurring in the plastometric tests. The general conclusion can be drawn that, when the inverse analysis is applied, obtained flow stress is a property of materials insensitive to the type of the test, sample dimensions etc. In consequence, accurate analysis of the influence of parameters, which really affect the flow stress (such as state of stress, preheating, etc), became possible. The investigation has also shown that conventional approach to the austenite microstructure evolution modelling, developed by Sellars (1979) and co-workers, is sufficient for accurate simulation of forging operations.

The results of the numerical simulation of forging process compare fairly well with the metallographic investigation results, which confirm a good predictive ability of the developed models. This refers to the flow pattern, as well as to the state of austenite microstructure in the forged element.

The approach adopted in the study can readily be extended for different steel grades to model the thermal-mechanical- and microstructural phenomena occurring during forging.

ACKNOWLEDGEMENTS

Financial assistance of MNiSzW, project no. R07 027 01, is acknowledged.

REFERENCES

Bariani, P., Bruschi, B., Ghiotti, A., 2007, Material testing and physical simulation in modelling process chains based on forging operations, *Computer Methods in Material Science*, 8, 378-382.

Chen, C.C., Kobayashi, S., 1978, Rigid plastic finite element analysis of ring compression, *Application of numerical methods to forming processes*, ASME, ADM, 28, 163-174.

Davenport, S.B., Silk, N.J., Sparks, C.N., Sellars, C.M., 1999, Development of constitutive equations for the modelling of hot rolling, *Mat. Sci. Techn*., 16, 1-8.

Gavrus, A., Massoni, E., Chenot, J.L., 1996, An inverse analysis using a finite element model for identification of rheological parameters, *J. Mat. Proc. Techn*., 60, 447-454.

Grosman, F., 1997, Application of the flow stress function in programmes for computer simulation of plastic working processes, *J. Mater. Proc. Technol*., 64, 169-180.

Karjalainen, L.P., Perttula, J., 1996, Characteristics of static and metadynamic recrystallization and strain accumulation in hot-deformed austenite as revealed by the stress relaxation method, *ISIJ International*, 36, 729-736

Kobayashi, S., Oh, S.I., Altan, T., 1989, *Metal forming and the finite element method*, Oxford University Press, New York, Oxford.

Kowalski, B., Sellars, C.M., Pietrzyk, M., 2000, Development of a computer code for the interpretation of results of hot plane strain compression tests, *ISIJ Int*., 40, 1230-1236.

Lee, C.H., Kobayashi, S., 1973, New solution to rigid plastic deformation problems, ASME, *J. Eng. Ind*., 95, 865-873.

Madej, Ł., Szeliga, D., Kuziak, R., Pietrzyk, M., 2007, Physical and numerical modelling of forging accounting for exploitation properties of products., *Computer Methods in Material Science*, 7, 397-405.

Ordon, J., Kuziak, R., Pietrzyk, M., 2000, History dependant constitutive law for austenitic steels, Proc. *Metal Forming 2000*, eds, Pietrzyk M., Kusiak J., Majta J., Hartley P., Pillinger I., Publ. A. Balkema, Kraków, 747-753.

Pietrzyk, M., 1994, Numerical aspects of the simulation of hot metal forming using internal variable method, *Metall. Foundry Eng*., 20, 429-439.

Pietrzyk, M., 2000, Finite element simulation of large plastic deformation, *J. Mat. Proc. Techn*., 106, 223-229.

Sandstrom, R., Lagneborg, R., 1975, A model for statc recrystallization after hot deformation, *Acta Metall*., 23, 481-488.

Szeliga, D., Gawąd, J., Pietrzyk, M., 2006a, Inverse analysis for identification of rheological and friction models in metal forming, *Comp. Meth. Appl. Mech. Engrg*., 195, 6778-6798.

Szeliga, D., Węglarczyk, S., Pietrzyk, M., 2006b, Estimation of simulation errors due to inaccurate evaluation of material properties in metal forming, *J. Machine Eng*., 6, 64-72.

Sellars, C.M., 1979, Physical metallurgy of hot working, *Hot working and forming processes*, eds, Sellars, C.M., Davies, G.J., *The Metals Soc*., London, 3-15.

FORGE 2008 Documentation, 2008, 3D Forging Datafile, Transvalor.

WERYFIKACJA CIEPLNO-MECHANICZNO-MIKROSTRUKTURALNEGO MODELU DLA PROCESU KUCIA NA GORĄCO

Streszczenie

W artykule przedstawiono wyniki badań dotyczących matematycznego modelowania procesu kucia, w warunkach powodujących szybkie zmiany temperatury materiału, umożliwiających przeprowadzenie obliczeń rozkładu efektywnego odkształcenia, prędkości odkształcenia i zmian mikrostruktury. Materiałem do badań była stal stopowa 16NCD13, dla której nie opracowano dotychczas modelu rozwoju mikrostruktury, zaś technologie kucia tej stali opracowywane były w oparciu o wiedzę inżynierską. Z tego powodu najważniejszym celem badań było opracowanie modelu reologicznego i rozwoju struktury dla tej stali. Modele te opracowano w oparciu o wyniki badań plastometrycznych, w trakcie których odkształcano próbki cylindryczne stosując szerokie przedziały zmienności prędkości odkształcenia i temperatury. Wyniki badań plastometrycznych w postaci zależności siły od przemieszczenia narzędzia poddano analizie odwrotnej, która wyeliminowała wpływ tarcia i nagrzewania adiabatycznego próbki na wartość naprężenia uplastyczniającego. W ten sposób otrzymano rzeczywiste krzywe naprężenie-odkształcenie, które posłużyły do opracowania modeli reologicznych charakteryzujących się różnym stopniem skomplikowania. W celu opracowania modelu zmian mikrostruktury austenitu zastosowano metodę relaksacji naprężenia oraz bezpośredniego chłodzenia próbki po odkształceniu. Próbki chłodzone wodą poddano ilościowej ocenie mikrostruktury. Opracowany model reologiczny i rozwoju mikrostruktury implementowano w programie Forge2008 i zastosowano do symulacji numerycznej procesu kucia odkuwki w warunkach przemysłowych. Wyniki przeprowadzonych symulacji dobrze korespondowały z wynikami badań metaloznawczych przeprowadzonych na odkuwkach, co wskazuje na poprawność opracowanych modeli.

Received: October 02, 2009
Received in a revised form: January 15, 2010
Accepted: January 18, 2010